PRAMANA — journal of physics

Vol. 82, No. 5
May 2014
pp. 809–822

Effective interaction: From nuclear reactions to neutron stars

D N BASU
Variable Energy Cyclotron Centre, 1/AF Bidhan Nagar, Kolkata 700 064, India
E-mail: dnb@vecc.gov.in

DOI: 10.1007/s12043-014-0734-5; ***e*Publication:** 30 April 2014

Abstract. An equation of state (EoS) for symmetric nuclear matter is constructed using the density-dependent M3Y effective interaction and extended for isospin asymmetric nuclear matter. Theoretically obtained values of symmetric nuclear matter incompressibility, isobaric incompressibility, symmetry energy and its slope agree well with experimentally extracted values. Folded microscopic potentials using this effective interaction, whose density dependence is determined from nuclear matter calculations, provide excellent descriptions for proton, alpha and cluster radioactivities, elastic and inelastic scattering. The nuclear deformation parameters extracted from inelastic scattering of protons agree well with other available results. The high density behaviour of symmetric and asymmetric nuclear matter satisfies the constraints from the observed flow data of heavy-ion collisions. The neutron star properties studied using β-equilibrated neutron star matter obtained from this effective interaction reconcile with the recent observations of the massive compact stars.

Keywords. Equation of state; neutron star; scattering; nuclear deformation; radioactivity.

PACS Nos 21.30.Fe; 21.65.−f; 25.40.−h; 23.50.+z; 23.60.+e; 23.70.+j; 26.60.−c

1. Introduction

The measurements of nuclear masses, densities and collective excitations have allowed to resolve some of the basic features of equation of state (EoS) of nuclear matter. However, the symmetry properties of EoS due to differing neutron and proton numbers remain more elusive to date and study of the isospin-dependent properties of asymmetric nuclear matter and the density dependence of the nuclear symmetry energy (NSE) have become the prime objective [1,2]. Consequently, the ultimate goal of such study is to extract information on the isospin dependence of in-medium nuclear effective interactions, as well as, the EoS of isospin asymmetric nuclear matter, particularly its isospin-dependent term or the density dependence of the NSE. This knowledge is important for understanding the structure of

radioactive nuclei, the reaction dynamics induced by rare isotopes, the liquid–gas phase transition in asymmetric nuclear matter and many critical issues in astrophysics [1–3].

In this work, based on the theoretical description of nuclear matter using the density-dependent M3Y-Reid–Elliott effective interaction [4,5] (DDM3Y), we carry out a systematic study of the symmetric nuclear matter (SNM) and isospin-dependent bulk properties of asymmetric nuclear matter. In particular, we study the density dependence of the NSE and extract the slope L and the curvature $K_{\rm sym}$ parameters of the NSE and the isospin-dependent part K_τ of the isobaric incompressibility.

The lifetimes of radioactive decays are calculated theoretically within the improved WKB approximation [6] using microscopic proton, α and nucleus–nucleus interaction potentials. These nuclear potentials have been obtained by folding the densities of the emitted and the daughter nuclei with the M3Y effective interaction, whose density dependence is determined from nuclear matter calculations. These calculations provide reasonable estimates of half-lives for the observed proton [7], α [8–11] and cluster [12] radioactivities. These folding model potentials provide excellent descriptions for elastic and inelastic scattering and the nuclear deformation parameters extracted from inelastic scattering of protons [13,14] agree well with other available results.

We present a systematic study of the properties of pure hadronic and hybrid compact stars. The nuclear EoS for β-equilibrated neutron star (NS) matter obtained using density-dependent effective nucleon–nucleon interaction satisfies the constraints from the observed flow data from heavy-ion collisions. The energy density of quark matter is lower than that of the nuclear EoS at higher densities implying possibility of transition to quark matter inside the core. We solve the Einstein's equations for rotating stars using pure nuclear matter and quark core. The β-equilibrated NS matter with a thin crust is able to describe highly massive compact stars [15] but it is found that the nuclear to quark matter deconfinement transition inside NSs causes reduction in their masses.

2. Effective interaction and its density dependence from nuclear matter calculations

The nuclear matter EoS is calculated using isoscalar and isovector [16] components of M3Y effective nucleon–nucleon interaction along with density dependence. The density dependence of the effective interaction, DDM3Y, is completely determined from nuclear matter calculations. The equilibrium density of the nuclear matter is determined by minimizing the energy per nucleon. The energy variation of the zero range potential is treated accurately by allowing it to vary freely with the kinetic energy part $\epsilon^{\rm kin}$ of the energy per nucleon ϵ over the entire range of ϵ. This is not only more plausible, but also yields excellent results for the incompressibility K_∞ of SNM which does not suffer from the superluminosity problem.

In a Fermi gas model of interacting neutrons and protons, with isospin asymmetry $X = (\rho_{\rm n} - \rho_{\rm p})/(\rho_{\rm n} + \rho_{\rm p})$, $\rho = \rho_{\rm n} + \rho_{\rm p}$ where $\rho_{\rm n}$, $\rho_{\rm p}$ and ρ are the neutron, proton and nucleonic densities, respectively, energy per nucleon for isospin asymmetric nuclear matter is given by [7]

$$\epsilon(\rho, X) = \left[\frac{3\hbar^2 k_{\rm F}^2}{10m}\right] F(X) + \left(\frac{\rho J_v C}{2}\right)(1 - \beta\rho^n), \tag{1}$$

where $k_F = (1.5\pi^2\rho)^{1/3}$ which equals Fermi momentum in case of SNM, the kinetic energy per nucleon $\epsilon^{kin} = [3\hbar^2 k_F^2/10m]F(X)$ with $F(X) = [((1+X)^{5/3} + (1-X)^{5/3})/2]$ and $J_v = J_{v00} + X^2 J_{v01}$, J_{v00} and J_{v01} represent the volume integrals of the isoscalar and the isovector parts of the M3Y interaction. The isoscalar t_{00}^{M3Y} and the isovector t_{01}^{M3Y} components of M3Y interaction potential are given by

$$t_{00}^{M3Y}(s,\epsilon) = 7999\frac{\exp(-4s)}{4s} - 2134\frac{\exp(-2.5s)}{2.5s} + J_{00}(1-\alpha\epsilon)\delta(s)$$

and

$$t_{01}^{M3Y}(s,\epsilon) = -4886\frac{\exp(-4s)}{4s} + 1176\frac{\exp(-2.5s)}{2.5s} + J_{01}(1-\alpha\epsilon)\delta(s)$$

with

$$J_{00} = -276 \text{ MeV fm}^3, \qquad J_{01} = 228 \text{ MeV fm}^3, \qquad \alpha = 0.005 \text{ MeV}^{-1}.$$

The DDM3Y effective *NN* interaction is given by $v_{0i}(s,\rho,\epsilon) = t_{0i}^{M3Y}(s,\epsilon)g(\rho)$, where the density dependence $g(\rho) = C(1-\beta\rho^n)$ with C and β being the constants of density dependence.

Equation (1) along with the saturation condition $(\partial\epsilon/\partial\rho) = 0$ at $X = 0$, $\rho = \rho_0$ and $\epsilon = \epsilon_0$ can be solved simultaneously for fixed values of the saturation energy per nucleon ϵ_0 and the saturation density ρ_0 of the cold SNM to obtain the values of β and C. The constants of density dependence β and C, thus obtained, are given by

$$\begin{aligned} \beta &= \frac{[(1-p)+(q-(3q/p))]\rho_0^{-n}}{[(3n+1)-(n+1)p+(q-(3q/p))]}, \\ p &= \frac{[10m\epsilon_0]}{[\hbar^2 k_{F_0}^2]}, \qquad q = \frac{2\alpha\epsilon_0 J_{00}}{J_{v00}^0}, \end{aligned} \tag{2}$$

where $J_{v00}^0 = J_{v00}(\epsilon_0^{kin})$ which means J_{v00} at $\epsilon^{kin} = \epsilon_0^{kin}$, the kinetic energy part of the saturation energy per nucleon of SNM, $k_{F_0} = [1.5\pi^2\rho_0]^{1/3}$ and

$$C = -\frac{\left[2\hbar^2 k_{F_0}^2\right]}{5mJ_{v00}^0\rho_0\left[1-(n+1)\beta\rho_0^n - \frac{q\hbar^2 k_{F_0}^2(1-\beta\rho_0^n)}{10m\epsilon_0}\right]}, \tag{3}$$

respectively. It is quite obvious that the constants of density dependence C and β obtained by this method depend on the saturation energy per nucleon ϵ_0, the saturation density ρ_0, the index n of the density-dependent part and on the strengths of the M3Y interaction through the volume integral J_{v00}^0.

The calculations are performed using the values of the saturation density $\rho_0 = 0.1533$ fm^{-3} [17] and the saturation energy per nucleon $\epsilon_0 = -15.26$ MeV [18] for the SNM obtained from the coefficient of the volume term of Bethe–Weizsäcker mass formula, which is evaluated by fitting the recent experimental and estimated atomic mass excesses from Audi–Wapstra–Thibault atomic mass table [19] by minimizing the mean square deviation, incorporating corrections for the electronic binding energy [20]. Using the usual values of $\alpha = 0.005$ MeV^{-1} for the parameter of energy dependence of zero range potential and $n = 2/3$, -15.26 ± 0.52 MeV for saturation energy per nucleon

(which is the volume energy coefficient a_v and covers, more or less, the entire range of values obtained for a_v [21]), values obtained for the constants of density dependence are $C = 2.2497 \pm 0.0420$, $\beta = 1.5934 \pm 0.0085$ fm^2 and that for SNM incompressibility is $K_\infty = 274.7 \pm 7.4$ MeV.

3. The equation of state

3.1 *Symmetric and asymmetric nuclear matter*

The EoSs of the symmetric and the asymmetric nuclear matter describing energy per nucleon as a function of nucleonic density can be obtained by setting $X = 0$ and non-zero, respectively, in eq. (1). The incompressibility or the compression modulus of SNM, which is a measure of curvature of an EoS at saturation density and defined as $k_F^2 \frac{\partial^2 \epsilon}{\partial k_F^2}|_{k_F = k_{F_0}}$, measures the stiffness of an EoS and obtained theoretically using eq. (1) for $X = 0$. The incompressibilities for isospin asymmetric nuclear matter are evaluated at saturation densities ρ_s with the condition $(\partial \epsilon / \partial \rho) = 0$ which corresponds to vanishing pressure. The incompressibility K_s for isospin asymmetric nuclear matter is therefore, expressed as

$$K_s = -\frac{3\hbar^2 k_{F_s}^2}{5m} F(X) - \frac{9 J_v^s C n (n+1) \beta \rho_s^{n+1}}{2} - 9\alpha J C [1 - (n+1)\beta \rho_s^n] \left[\frac{\rho_s \hbar^2 k_{F_s}^2}{5m} \right] F(X) + \left[\frac{3\rho_s \alpha J C (1 - \beta \rho_s^n) \hbar^2 k_{F_s}^2}{10m} \right] F(X). \quad (4)$$

Here, k_{F_s} means that k_F is evaluated at the saturation density ρ_s. $J_v^s = J_{v00}^s + X^2 J_{v01}^s$ is J_v at $\epsilon^{kin} = \epsilon_s^{kin}$, which is the kinetic energy part of the saturation energy per nucleon ϵ_s and $J = J_{00} + X^2 J_{01}$.

In table 1, incompressibility of isospin asymmetric nuclear matter K_s as a function of the isospin asymmetry parameter X is provided. The magnitude of the incompressibility K_s decreases with the isospin asymmetry X due to lowering of the saturation densities

Table 1. Incompressibility of isospin asymmetric nuclear matter using $\rho_0 = 0.1533$ fm^{-3}, $\epsilon_0 = -15.26$ MeV, $n = 2/3$ and $\alpha = 0.005$ MeV^{-1}.

X	ρ_s (fm^{-3})	K_s (MeV)
0.0	0.1533	274.7
0.1	0.1525	270.4
0.2	0.1500	257.7
0.3	0.1457	236.6
0.4	0.1392	207.6
0.5	0.1300	171.2

ρ_s with X, as well as, decrease in the EoS curvature. At high isospin asymmetry X, the isospin asymmetric nuclear matter does not have a minimum, signifying that it can never be bound by itself due to nuclear interaction. However, the β equilibrated nuclear matter which is highly neutron-rich asymmetric nuclear matter exists in the core of NSs since its E/A is lower than that of SNM at high densities and is unbound by the nuclear force, but can be bound due to high gravitational field realizable inside NSs.

It is interesting to note that the RMF-NL3 incompressibility for SNM is 271.76 MeV [22] which is about the same as 274.7±7.4 MeV obtained from the present calculation. The recent acceptable value [23,24] of SNM incompressibility lies in the range of 250–270 MeV and the calculated value of 274.7±7.4 MeV is a good theoretical result and is only slightly too high. Although, parameters of the density dependence of DDM3Y interaction have been tuned to reproduce ρ_0 and ϵ_0, which are obtained from finite nuclei, the agreement of the present EoS with the experimental flow data [3], where the high density behaviour looks phenomenologically confirmed, justifies its extrapolation to high density.

3.2 *Incompressibility, isobaric incompressibility, symmetry energy and its slope*

The EoS of isospin asymmetric nuclear matter, given by eq. (1) can be expanded in general as

$$\epsilon(\rho, X) = \epsilon(\rho, 0) + E_{\rm sym}(\rho)X^2 + O(X^4) \tag{5}$$

and

$$E_{\rm sym}(\rho) = \frac{1}{2}\frac{\partial^2\epsilon(\rho, X)}{\partial X^2}\bigg|_{X=0}$$

is termed as the NSE. The absence of odd-order terms in X in eq. (5) is due to the exchange symmetry between protons and neutrons in nuclear matter when one neglects the Coulomb interaction and assumes the charge symmetry of nuclear forces. The higher-order terms in X are negligible and to a good approximation, the density-dependent NSE $E_{\rm sym}(\rho)$ can be extracted using the following equation [25]:

$$E_{\rm sym}(\rho) = \epsilon(\rho, 1) - \epsilon(\rho, 0) \tag{6}$$

which can be obtained using eq. (1) and represents a penalty levied on the system as it departs from the symmetric limit of equal number of protons and neutrons and can be defined as the energy required per nucleon to change SNM to pure neutron matter (PNM).

The volume symmetry energy coefficient S_v extracted from nuclear masses provides a constraint on the NSE at nuclear density $E_{\rm sym}(\rho_0)$. The value of $S_v = 30.048\pm0.004$ MeV extracted [26] from the measured atomic mass excesses of 2228 nuclei is reasonably close to the theoretical estimate of the value of NSE at saturation density $E_{\rm sym}(\rho_0)$=30.71±0.26 MeV obtained from the present calculations using DDM3Y interaction. If one uses the alternative definition of

$$E_{\rm sym}(\rho) = \frac{1}{2}\frac{\partial^2\epsilon(\rho, X)}{\partial X^2}\bigg|_{X=0},$$

the value of NSE at saturation density remains almost the same which is 30.03±0.26 MeV. Empirically, the value of $E_{\rm sym}(\rho_0) \approx 30$ MeV [2,27,28] seems well established. Theoretically different parametrizations of the relativistic mean-field (RMF) models, which

fit observables for isospin symmetric nuclei well, lead to a relatively wide range of predictions of 24–40 MeV for $E_{\rm sym}(\rho_0)$. The present result of 30.71±0.26 MeV is close to that using Skyrme interaction SkMP (29.9 MeV) [29] and Av18 + δv + UIX* variational calculation (30.1 MeV) [30].

Around the nuclear matter saturation density ρ_0, the NSE $E_{\rm sym}(\rho)$ can be expanded to second order in density as

$$E_{\rm sym}(\rho) = E_{\rm sym}(\rho_0) + \frac{L}{3}\left(\frac{\rho-\rho_0}{\rho_0}\right) + \frac{K_{\rm sym}}{18}\left(\frac{\rho-\rho_0}{\rho_0}\right)^2, \tag{7}$$

where L and $K_{\rm sym}$ represents the slope and curvature parameters of NSE at ρ_0 and hence,

$$L = 3\rho_0 \frac{\partial E_{\rm sym}(\rho)}{\partial \rho}\bigg|_{\rho=\rho_0} \quad \text{and} \quad K_{\rm sym} = 9\rho_0^2 \frac{\partial^2 E_{\rm sym}(\rho)}{\partial \rho^2}\bigg|_{\rho=\rho_0}.$$

L and $K_{\rm sym}$ characterize the density dependence of the NSE around normal nuclear matter density and thus, carry important information on the properties of NSE at both high and low densities. In particular, the slope parameter L has been found to correlate linearly with the neutron-skin thickness of heavy nuclei and can be determined from the measured thickness of neutron skin of such nuclei [31]. The isobaric incompressibility for infinite nuclear matter can be expanded in the power series of isospin asymmetry X as $K_\infty(X) = K_\infty + K_\tau X^2 + K_4 X^4 + O(X^6)$. The magnitude of the higher-order K_4 parameter is generally quite small compared to K_τ [32]. The latter characterizes the isospin dependence of the incompressibility at saturation density and can be expressed as

$$K_\tau = K_{\rm sym} - 6L - \frac{Q_0}{K_\infty}L = K_{\rm asy} - \frac{Q_0}{K_\infty}L,$$

where Q_0 is the third-order derivative parameter of SNM at ρ_0 given by

$$Q_0 = 27\rho_0^3 \frac{\partial^3 \epsilon(\rho,0)}{\partial \rho^3}\bigg|_{\rho=\rho_0}.$$

In table 2, the values of K_∞, $E_{\rm sym}(\rho_0)$, L, $K_{\rm sym}$ and K_τ are listed and compared with the corresponding quantities obtained with relativistic mean field (RMF) models [33]. In figure 1, K_τ is plotted against K_∞ for the present calculation using DDM3Y interaction and compared with the predictions of FSUGold, NL3, Hybrid [33], SkI3, SkI4, SLy4,

Table 2. Results of present calculations (DDM3Y) for SNM incompressibility K_∞, nuclear symmetry energy $E_{\rm sym}(\rho_0)$, slope L and curvature $K_{\rm sym}$ of nuclear symmetry energy, approximate isospin-dependent part $K_{\rm asy}$ and exact part K_τ of isobaric incompressibility (all in MeV) compared with those obtained with RMF models [33].

Model	K_∞	$E_{\rm sym}(\rho_0)$	L	$K_{\rm sym}$	$K_{\rm asy}$	Q_0	K_τ
Present work	274.7	30.71	45.11	−183.7	−454.4	−276.5	−408.97
	±7.4	±0.26	±0.02	±3.6	±3.5	±10.5	±3.01
FSUGold	230.0	32.59	60.5	−51.3	−414.3	−523.4	−276.77
NL3	271.5	37.29	118.2	+100.9	−608.3	+204.2	−697.36
Hybrid	230.0	37.30	118.6	+110.9	−600.7	−71.5	−563.86

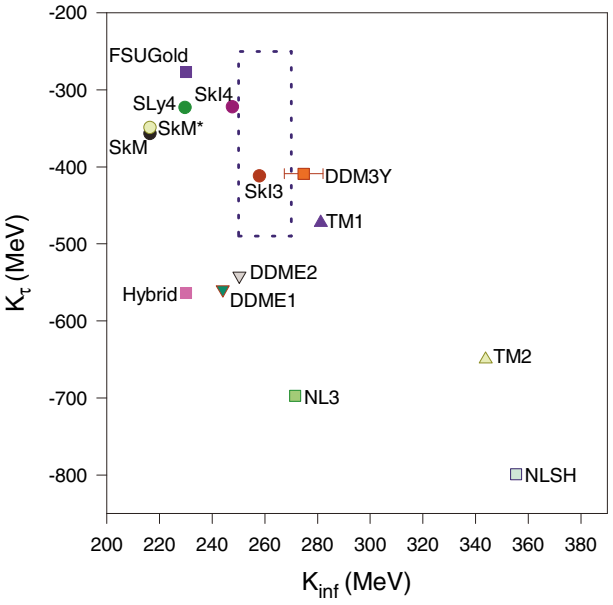

Figure 1. K_τ is plotted against K_∞ ($K_{\rm inf}$) for present calculations using DDM3Y interactions and compared with other predictions [33,34]. The dotted rectangular region encompasses the values of $K_\infty = 250$–270 MeV [24] and $K_\tau = -370\pm120$ MeV [32].

SkM, SkM*, NLSH, TM1, TM2, DDME1 and DDME2 as given in table 1 of [34]. The dotted rectangular region encompasses the recent values of $K_\infty = 250$–270 MeV [24] and $K_\tau = -370\pm120$ MeV [32]. Although both DDM3Y and SkI3 are within the above region, unlike DDM3Y the L value for SkI3 is 100.49 MeV which is much above the acceptable limit of 45–75 MeV [35] whereas DDME2 which gives $L = 51$ MeV is reasonably close to the rectangular region. Present NSE is 'super-soft' because it increases initially with nucleonic density up to about two times the normal nuclear density and then decreases monotonically (hence 'soft') and becomes negative (hence 'supersoft') at higher densities (about 4.7 times the normal nuclear density) [7,36] and is consistent with recent evidence for a soft NSE at suprasaturation densities [37] and with the fact that supersoft nuclear symmetry energy preferred by the FOPI/GSI experimental data on π^+/π^- ratio in relativistic heavy-ion reactions can readily keep NSs stable if the non-Newtonian gravity proposed in the grand unification theories is considered [38].

4. Nuclear scattering

4.1 *Elastic scattering using potentials from folding effective interaction*

The microscopic proton–nucleus interaction potentials are obtained by single folding the density distribution of the nucleus with the DDM3Y effective interaction as

$$V_N(R) = \int \rho(\vec{r}) v_{00}(|\vec{R} - \vec{r}|) \mathrm{d}^3\vec{r}, \tag{8}$$

where $\rho(\vec{r})$ is the density of the nucleus at $\vec{r}$ and v_{00} is the effective interaction between two nucleons at the sites $\vec{R}$ and $\vec{r}$. The parameters of the density dependence, $C = 2.2497$ and $\beta = 1.5934$ fm^2, used here are obtained from the nuclear matter calculations. The nuclear ground state densities are calculated in the framework of spherical Hartree–Fock plus BCS calculations in coordinate space using SkM* [39] parametrization and used for calculating $V_N(R)$ and form factor. Phenomenological optical potentials have the form

$$V_{\text{pheno}}(r) = -V_{\text{o}} f_{\text{o}}(r) - iW_{\text{v}} f_{\text{v}}(r) + 4ia_{\text{s}} W_{\text{s}} \frac{\text{d}f_{\text{s}}(r)}{\text{d}r} + 2\left(\frac{\hbar}{m_\pi c}\right)^2 V_{\text{so}} \left(\frac{1}{r}\right) \frac{\text{d}f_{\text{so}}(r)}{\text{d}r}(\text{LS}) + V_{\text{coul}},$$

where

$$f_x(r) = \left[1 + \exp\left(\frac{r - R_x}{a_x}\right)\right]^{-1}, \qquad R_x = r_x A^{1/3}$$

and x = o, v, s, so. The subscripts o, v, s, so denote real, volume imaginary, surface imaginary and spin-orbit, respectively and V_{o}, $W_{\text{v}}(W_{\text{s}})$ and V_{so} are the strengths of real, volume (surface) imaginary and spin-orbit potentials, respectively. V_{coul} is the Coulomb potential of a uniformly charged sphere of radius $1.20A^{1/3}$. In semimicroscopic analysis, both the volume real (V) and volume imaginary (W) parts of the potentials (generated microscopically by folding model) are assumed to have the same shape, i.e., $V_{\text{micro}}(r) = V + iW = (N_{\text{R}} + iN_{\text{I}})V_{\text{N}}(r)$, where N_{R} and N_{I} are the renormalization factors for real and imaginary parts, respectively [40]. Thus, the potentials for elastic scattering analysis include real and volume imaginary terms (folded potentials) and also surface imaginary and spin-orbit terms (best-fit phenomenological potentials). Best fits are obtained by minimizing

$$\frac{\chi^2}{N} = \frac{1}{N} \sum_{k=1}^{N} \left[\frac{\sigma_{\text{th}}(\theta_k) - \sigma_{\text{ex}}(\theta_k)}{\Delta\sigma_{\text{ex}}(\theta_k)}\right]^2$$

for each angular distribution, where σ_{th}, σ_{ex} are theoretical and experimental cross-sections, respectively, at angle θ_k, $\Delta\sigma_{\text{ex}}$ is the experimental error and N is the number of data points.

4.2 *Inelastic scattering and nuclear deformation parameter*

The potentials for elastic scattering analysis are subsequently used in the DWBA calculations of inelastic scattering with transferred angular momentum l. The calculations are performed using the code DWUCK4 [41]. The derivative of the potentials ($\delta(\text{d}V/\text{d}r)$) are used as the form factors. The microscopic real and imaginary form factors have the same shape with strengths N_{R}^{FF} and N_{I}^{FF}, respectively. Here, $N_{\text{R,I}}^{\text{FF}} = N_{\text{R,I}} r_{\text{rms}}^{V}$, where r_{rms}^{V} is the rms radius of the folded potential. In addition, form factors derived from phenomenological surface imaginary and spin-orbit potentials are included. The deformation parameters δ are determined by fitting the inelastic scattering angular distribution. Table 3 shows that the quadrupole deformations obtained from the present analysis for ^{18,20,22}O are in excellent agreement with those extracted from $B(E2)$ values [42] while that for ^{18}Ne is significantly underestimated due to lack of experimental data at forward angles.

Table 3. Comparison of nuclear deformation parameters δ extracted from inelastic scattering and from $B(E2)$ values.

Nucleus	δ (Present work)	δ (From $B(E2)$ values)
O^{18}	0.33	0.355(8)[a]
O^{20}	0.46	0.261(9)[a] [0.50(4)[b]]
O^{22}	0.26	0.208(41)[a]
Ne^{18}	0.40	0.694(34)[a]

[a] [42].
[b] [43].

5. Nuclear decays

5.1 *Proton radioactivity*

The half-lives of the decays of spherical nuclei away from proton drip line by proton emissions are estimated theoretically. The half-life of a parent nucleus decaying via proton emission is calculated using the WKB barrier penetration probability. The WKB method is found quite satisfactory and even better than the S-matrix method for calculating half-widths of the α decay of superheavy elements [44]. For the present calculations, the zero point vibration energies used are given by eq. (5) [45] extended to protons and the experimental Q values [46] are used. Spherical charge distributions are used for Coulomb interaction potentials. The nuclear potential $V_{\rm N}(R)$ of eq. (8) has been replaced by $V_{\rm N}(R) + V_N^{\rm Lane}(R)$, where the isovector [16] or symmetry component of the folded potential $V_{\rm N}^{\rm Lane}(R) = \int\int[\rho_{1n}(\vec{r}_1) - \rho_{1p}(\vec{r}_1)][\rho_{2n}(\vec{r}_2) - \rho_{2p}(\vec{r}_2)]v_{01}[|\vec{r}_2 - \vec{r}_1 + \vec{R}|]{\rm d}^3r_1{\rm d}^3r_2$, where the subscripts 1 and 2 denote the daughter and the emitted nuclei, respectively, while the subscripts n and p denote neutron and proton densities, respectively. With a simple assumption that

$$\rho_{1p} = \left[\frac{Z_{\rm d}}{A_{\rm d}}\right]\rho \qquad \text{and} \qquad \rho_{1n} = \left[\frac{(A_{\rm d} - Z_{\rm d})}{A_{\rm d}}\right]\rho,$$

and for the emitted particle being proton

$$\rho_{2n}(\vec{r}_2) - \rho_{2p}(\vec{r}_2) = -\rho_2(\vec{r}_2) = -\delta(\vec{r}_2),$$

the Lane potential becomes

$$V_{\rm N}^{\rm Lane}(R) = -\left[\frac{(A_{\rm d} - 2Z_{\rm d})}{A_{\rm d}}\right]\int \rho(\vec{r})v_{01}[|\vec{r} - \vec{R}|]{\rm d}^3r,$$

where $v_{01}(s) = t_{01}^{\rm M3Y}(s, E)g(\rho)$ and $A_{\rm d}$ and $Z_{\rm d}$ are, respectively, the mass number and the charge number of the daughter nucleus. The inclusion of this Lane potential causes insignificant changes in the lifetimes. The same set of data of [47] has been used for the present calculations using $C = 2.2497$ and $\beta = 1.5934$ fm^2. The agreement of the present calculations with a wide range of experimental data for the proton radioactivity lifetimes are reasonably good [7].

5.2 α *radioactivity of SHE*

The double-folded nuclear potential between the daughter and emitted nuclei is given by

$$V_{\mathrm{N}}(R) = \int\int \rho_1(\vec{r}_1)\rho_2(\vec{r}_2)v_{00}[|\vec{r}_2 - \vec{r}_1 + \vec{R}|]\mathrm{d}^3r_1\mathrm{d}^3r_2, \tag{9}$$

where ρ_1, ρ_2 are the density distribution functions for the two composite nuclear fragments. Since the density dependence of the effective projectile–nucleon interaction was found to be fairly independent of the projectile [48], as long as the projectile–nucleus interaction was amenable to a single-folding prescription, the density-dependent effects on the nucleon–nucleon interaction can be factorized into a target term times a projectile term as $g(\rho_1, \rho_2) = C(1 - \beta\rho_1^{2/3})(1 - \beta\rho_2^{2/3})$. The parameter β can be related to the mean free path in nuclear medium; hence its value should remain the same, 1.5934 fm^2, as that obtained from nuclear matter calculations, while the other constant C, which is basically an overall normalization constant, may change. The value of this overall normalization constant is kept equal to unity, which has been found to be $\approx$1 from an optimum fit to a large number of α decay lifetimes [8]. This formulation is used successfully in the case of α radioactivity of nuclei [8] including superheavies [9–11]. In α decay calculations only the isoscalar term contributes because α contains equal number of neutrons and protons.

5.3 *Cluster radioactivity*

The decay constant λ for cluster radioactivity is a product of cluster preformation probability P_0 in the ground state, the tunnelling probability through barrier P and the assault frequency ν. The preformation factor may be considered as the overlap of the actual ground state configuration and the configuration representing the cluster coupled to the ground state of the daughter. Superheavy emitters being loosely bound compared to highly bound α, P_0 is expected to be high for α decay and the present calculations with $P_0 = 1$ provide excellent description of α decay for recently discovered superheavy nuclei [9–11]. For weakly bound heavy cluster decay it is expected to be orders of magnitude less than unity. The theoretical half-lives of cluster radioactivity for very heavy nuclei are calculated by assuming the cluster preformation factor to be unity. Hence, the preformation factors P_0 are calculated [12] as the ratios of the calculated half-lives to the experimentally observed half-lives.

6. Neutron stars

6.1 *Modelling neutron stars*

If rapidly rotating compact stars were nonaxisymmetric, they would emit gravitational waves in a very short time-scale and settle down to axisymmetric configurations. Therefore, we need to solve for rotating and axisymmetric configurations in the framework of general relativity. For the matter and the space-time the following assumptions are made: (a) the matter distribution and the space-time are axisymmetric, (b) the matter and the space-time are in a stationary state, (c) the matter has no meridional motions, (d) the only motion of the matter is a circular one that is represented by the angular velocity, (e) the

angular velocity is constant as seen by a distant observer at rest and (f) the matter can be described as a perfect fluid. The energy–momentum tensor of a perfect fluid $T^{\mu\nu}$ is given by $T^{\mu\nu} = (\varepsilon + P)u^\mu u^\nu - g^{\mu\nu}P$, where ε, P, u^μ and $g^{\mu\nu}$ are the energy density, pressure, four-velocity and the metric tensor, respectively. To study the rotating stars, the following metric is used:

$$\mathrm{d}s^2 = -\mathrm{e}^{(\gamma+\rho)}\mathrm{d}t^2 + \mathrm{e}^{2\alpha}(\mathrm{d}r^2 + r^2\mathrm{d}\theta^2) + \mathrm{e}^{(\gamma-\rho)}r^2\sin^2\theta(\mathrm{d}\phi - \omega\mathrm{d}t)^2, \quad (10)$$

where gravitational potentials γ, ρ, α and ω are functions of polar coordinates r, θ. Einstein's field equations for the three potentials γ, ρ and α are solved using the Green's-function technique [49] and the fourth potential ω is determined from other potentials. At zero frequency limit corresponding to the static solutions of Einstein's field equations for spheres of fluid, the present formalism yields results for the solution of Tolman–Oppenheimer–Volkoff (TOV) equation [50].

6.2 *β-equilibrated neutron star matter and quark matter EoS*

The nuclear matter EoS, as described earlier, is calculated [7] using the isoscalar and the isovector components of M3Y interaction along with density dependence which is determined completely from the nuclear matter calculations. This EoS evaluated at the isospin asymmetry X determined from the β-equilibrium proton fraction x_β [$= (\rho_\mathrm{p}/\rho)$], obtained by solving $\hbar c(3\pi^2\rho x_\beta)^{1/3} = 4E_\mathrm{sym}(\rho)(1-2x_\beta)$, provides EoS for the β-equilibrated NSs matter, where $E_\mathrm{sym}(\rho)$ is the NSE. For cold and dense quark (QCD) matter, the perturbative EoS [51] with two massless and one massive quark flavours and a running coupling constant, is used. The constant B is treated as a free parameter, which allows to take into account nonperturbative effects not captured by the weak coupling expansion.

6.3 *Deconfinement phase transition: From nuclear matter to quark matter*

The energy density of the quark matter is lower than that of the present EoS for the β-equilibrated charge neutral NSs matter at densities higher than 0.405 fm^{-3} for bag constant $B^{1/4} = 110$ MeV [51] implying the presence of quark core. For lower values of bag constant such as $B^{1/4} = 89$ MeV, energy density for EoS is lower and makes a crossover with the quark matter EoS at very high density, $\sim$1.2 fm^{-3}, causing too little quark core (predicting similar results as NSs with pure nuclear matter inside) and therefore we choose $B^{1/4} = 110$ MeV for representative calculations. The common tangent is drawn for the energy density vs. density plots where pressure is the negative intercept of the tangent to energy density vs. density plot. However, the phase coexistence region is negligibly small which is represented by a part of the common tangent between the points of contact on the two plots [52] implying constant pressure throughout the phase transition.

6.4 *Calculations and results: Masses and radii of neutron and hybrid stars*

We use the 'rns' code [53] for calculating compact star properties which requires EoS in the form of energy density vs. pressure along with corresponding enthalpy and baryon number density. The rotating compact star calculations are performed using the crustal

EoS, FMT [54] + BPS [55] + BBP [56] upto the number density of 0.0458 fm^{-3} and β-equilibrated NS matter beyond. It is worthwhile to mention here that a star may not rotate as fast as Keplerian frequency due to r-mode instability. The variation of mass with central density for static and rotating NSs at Keplerian limit and also maximum frequencies limited by the r-mode instability with pure nuclear matter inside is shown in figure 2. For NSs with pure nuclear matter inside, the maximum mass for the static case is $1.92M_{\odot}$ with radius ∼9.7 km and for the star rotating with Kepler's frequency it is $2.27M_{\odot}$ with equatorial radius ∼13.1 km [57]. However, for stars rotating with maximum frequency limited by the r-mode instability, the maximum mass turns out to be 1.95 (1.94)$M_{\odot}$ corresponding to rotational period of 1.5 (2.0) ms with radius about 9.9 (9.8) km. When quark core is considered, the maximum mass for the static case is $1.68M_{\odot}$ with radius ∼10.4 km and for the star rotating with Kepler's frequency it is $2.02M_{\odot}$ with equatorial radius ∼14.3 km whereas stars rotating with maximum frequency limited by the r-mode instability, the maximum mass turns out to be 1.72 (1.71)$M_{\odot}$ corresponding to rotational period of 1.5 (2.0) ms with radius about 10.7 (10.6) km [58].

7. Summary and conclusions

In summary, we show that theoretical description of nuclear matter based on mean-field calculations using density-dependent M3Y effective NN interaction yields a value of nuclear incompressibility which is in good agreement with that extracted from experiment and gives a value of NSE that is consistent with the empirical value extracted by fitting the droplet model to the measured atomic mass excesses and with other modern theoretical descriptions of nuclear matter. The slope L and the isospin-dependent part K_{τ} of the isobaric incompressibility are consistent with the constraints recently extracted from the analyses of experimental data. We have applied our nucleonic EoS with a thin crust to solve the Einstein's field equations to determine the mass–radius relationship of

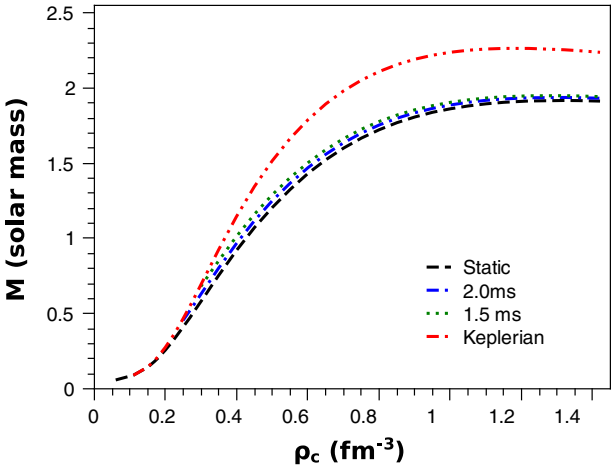

Figure 2. Variation of mass with central density for static and rotating NSs with pure nuclear matter inside.

NSs with and without quark cores. We have obtained the masses of neutron (hybrid) stars rotating with Keplerian frequencies, around 2.27 (2.02)$M_\odot$ with equatorial radii around 13 (14) km. The maximum mass of NS without quark core, with maximum rotational frequency limited by the *r*-mode instability, turns out to be 1.95 (1.94)$M_\odot$ corresponding to the rotational period of 1.5 (2.0) ms with radius about 9.9 (9.8) km which is in excellent agreement with recent astrophysical observations. The nucleon–nucleon effective interaction used in the present work, which is found to provide a unified description of elastic and inelastic scattering, various radioactivities and nuclear matter properties, also provide an excellent description of the β-equilibrated NS matter which is stiff enough at high densities to reconcile with the recent observations of the massive compact stars $\sim 2M_\odot$, while the corresponding symmetry energy is supersoft [36] as preferred by the FOPI/GSI experimental data.

References

[1] B A Li, L W Chen and C M Ko, *Phys. Rep.* **464**, 113 (2008)
[2] A W Steiner, M Prakash, J M Lattimer and P J Ellis, *Phys. Rep.* **411**, 325 (2005)
[3] P Danielewicz, R Lacey and W G Lynch, *Science* **298**, 1592 (2002)
[4] G Bertsch, J Borysowicz, H McManus and W G Love, *Nucl. Phys. A* **284**, 399 (1977)
[5] G R Satchler and W G Love, *Phys. Rep.* **55**, 183 (1979)
[6] E C Kemble, *Phys. Rev.* **48**, 549 (1935)
[7] D N Basu, P Roy Chowdhury and C Samanta, *Nucl. Phys. A* **811**, 140 (2008)
[8] D N Basu, *Phys. Lett. B* **566**, 90 (2003)
[9] P Roy Chowdhury, C Samanta and D N Basu, *Phys. Rev. C* **73**, 014612 (2006); ibid, *Phys. Rev. C* **77**, 044603 (2008); ibid, *At. Data Nucl. Data Tables* **94**, 781 (2008)
[10] P Roy Chowdhury, D N Basu and C Samanta, *Phys. Rev. C* **75**, 047306 (2007)
[11] C Samanta, P Roy Chowdhury and D N Basu, *Nucl. Phys. A* **789**, 142 (2007)
[12] T R Routray, Jagajjaya Nayak and D N Basu, *Nucl. Phys. A* **826**, 223 (2009)
[13] D Gupta and D N Basu, *Nucl. Phys. A* **748**, 402 (2005)
[14] D Gupta, E Khan and Y Blumenfeld, *Nucl. Phys. A* **773**, 230 (2006)
[15] P B Demorest, T Pennucci, S M Ransom, M S E Roberts and J W T Hessels, *Nature* **467**, 1081 (2010)
[16] A M Lane, *Nucl. Phys.* **35**, 676 (1962)
[17] C Samanta, D Bandyopadhyay and J N De, *Phys. Lett. B* **217**, 381 (1989)
[18] P Roy Chowdhury and D N Basu, *Acta Phys. Pol. B* **37**, 1833 (2006)
[19] G Audi, A H Wapstra and C Thibault, *Nucl. Phys. A* **729**, 337 (2003)
[20] D Lunney, J M Pearson and C Thibault, *Rev. Mod. Phys.* **75**, 1021 (2003)
[21] G Royer and C Gautier, *Phys. Rev. C* **73**, 067302 (2006)
[22] G A Lalazissis, S Raman and P Ring, *At. Data Nucl. Data Tables* **71**, 1 (1999)
[23] D Vretenar, T Nikšić and P Ring, *Phys. Rev. C* **68**, 024310 (2003)
[24] M M Sharma, *Nucl. Phys. A* **816**, 65 (2009)
[25] T Klähn *et al*, *Phys. Rev. C* **74**, 035802 (2006)
[26] T Mukhopadhyay and D N Basu, *Nucl. Phys. A* **789**, 201 (2007)
[27] P Danielewicz, *Nucl. Phys. A* **727**, 233 (2003)
[28] K Pomorski and J Dudek, *Phys. Rev. C* **67**, 044316 (2003)
[29] L Bennour *et al*, *Phys. Rev. C* **40**, 2834 (1989)
[30] A Akmal, V R Pandharipande and D G Ravenhall, *Phys. Rev. C* **58**, 1804 (1998)
[31] M Centelles, X Roca-Maza, X Vinas and M Warda, *Phys. Rev. Lett.* **102**, 122502 (2009)

[32] Lie-Wen Chen, Bao-Jun Cai, Che Ming Ko, Bao-An Li, Chun Shen and Jun Xu, *Phys. Rev. C* **80**, 014322 (2009)
[33] J Piekarewicz and M Centelles, *Phys. Rev. C* **79**, 054311 (2009)
[34] Hiroyuki Sagawa, Satoshi Yoshida, Guo-Mo Zeng, Jian-Zhong Gu and Xi-Zhen Zhang, *Phys. Rev. C* **76**, 034327 (2007)
[35] M Warda, X Viñas, X Roca-Maza and M Centelles, *Phys. Rev. C* **80**, 024316 (2009)
[36] P Roy Chowdhury, D N Basu and C Samanta, *Phys. Rev. C* **80**, 011305(R) (2009) D N Basu, P Roy Chowdhury and C Samanta, *Phys. Rev. C* **80**, 057304 (2009)
[37] Zhigang Xiao, Bao-An Li, Lie-Wen Chen, Gao-Chan Yong and Ming Zhang, *Phys. Rev. Lett.* **102**, 062502 (2009)
[38] De-Hua Wen, Bao-An Li and Lie-Wen Chen, *Phys. Rev. Lett.* **103**, 211102 (2009)
[39] J Bartel, P Quentin, M Brack, C Guet and H B Hakansson, *Nucl. Phys. A* **386**, 79 (1982)
[40] C Samanta, Y Sakuragi, M Ito and M Fujiwara, *J. Phys. G: Nucl. Part. Phys.* **23**, 1697 (1997)
[41] P D Kunz, computer code DWUCK4, unpublished
[42] S Raman *et al*, *At. Data Nucl. Data Tables* **78**, 1 (2001)
[43] J K Jewell *et al*, *Phys. Lett. B* **454**, 191 (1999)
[44] S Mahadevan, P Prema, C S Shastry and Y K Gambhir, *Phys. Rev. C* **74**, 057601 (2006)
[45] D N Poenaru, W Greiner, M Ivascu, D Mazilu and I H Plonski, *Z. Phys. A* **325**, 435 (1986)
[46] A A Sonzogni, *Nucl. Data Sheets* **95**, 1 (2002)
[47] M Balasubramaniam and N Arunachalam, *Phys. Rev. C* **71**, 014603 (2005)
[48] D K Srivastava, D N Basu and N K Ganguly, *Phys. Lett. B* **124**, 6 (1983)
[49] H Komatsu, Y Eriguchi and I Hachisu, *Mon. Not. R. Astron. Soc.* **237**, 355 (1989)
[50] R C Tolman, *Phys. Rev.* **55**, 364 (1939)
J R Oppenheimer and G M Volkoff, *Phys. Rev*. **55**, 374 (1939)
[51] A Kurkela, P Romatschke and A Vuorinen, *Phys. Rev. D* **81**, 105021 (2010)
[52] H Heiselberg, C J Pethick and E F Staubo, *Phys. Rev. Lett.* **70**, 1355 (1993)
[53] N Stergioulas and J L Friedman, *Astrophys. J.* **444**, 306 (1995)
[54] R P Feynman, N Metropolis and E Teller, *Phys. Rev*. **75**, 1561 (1949)
[55] G Baym, C J Pethick and P Sutherland, *Astrophys. J.* **170**, 299 (1971)
[56] G Baym, H A Bethe and C J Pethick, *Nucl. Phys. A* **175**, 225 (1971)
[57] P R Chowdhury, A Bhattacharyya and D N Basu, *Phys. Rev. C* **81**, 062801(R) (2010)
[58] Abhishek Mishra, P R Chowdhury and D N Basu, *Astropart. Phys.* **36**, 42 (2012)